An MTPA Tracking Method for Cost-Effective Mono-Inverter Multi PMSM Electric Drives

Ivan Spina, *Member, IEEE*, Gianluca Brando, Adolfo Dannier, *Senior Member, IEEE*, and Andrea Cervone, *Member, IEEE*

***Abstract*—Single-inverter multi-motor architectures offer the potential for significant system simplification, leading to a substantial reduction in required components. This results in a more cost-effective, lightweight, and compact structure. While this approach has been widely studied for Induction Motors and, to some extent, for two parallel-connected Permanent Magnet Synchronous Motors (PMSMs), the case of multiple PMSMs remains in its early stages of research. This paper contributes to advancing the study of optimized control strategies for Single-Inverter Multi-PMSM systems by proposing an innovative method for Maximum Torque Per Ampere (MTPA) point tracking suitable for implementation of a low-cost control platform. This method, here named Distributed Real-Time Computation (DRTC), is compared against a Perturb & Observe (P&O) approach in several operating conditions, including scenarios with motor parameter deviations. The optimal trajectories are investigated, and the impact of parameter variations is examined. The performance of the methods is evaluated through extensive numerical simulations and experimental validation. A comparative analysis of the results highlights the advantages and limitations of each method, demonstrating their effectiveness in tracking the optimal operating point under both steady-state and transient conditions, as well as in the presence of motor parameter variations.**

***Index Terms*—Loss minimization, maximum torque per ampere, permanent magnet synchronous motors (PMSMs), single inverter multi motor.**

I. Introduction

MONO-INVERTER Multi-Motor (MIMM) architectures reduce system complexity by minimizing the number of required components. Historically, the Induction Motor (IM) was the first electrical machine integrated into MIMM systems ([1], [2]), primarily due to its inherent self-stabilization and the ability to tolerate slip relative to the voltage frequency. This characteristic has made IMs suitable for various applications, including traction systems ([3], [4]), where differences in wheel diameters can be accommodated by variations in slip. Conversely, Permanent Magnet Synchronous Motors (PMSMs) operate strictly in synchronism with the inverter voltage frequency, presenting an inherent stability challenge when two or more PMSMs are connected in parallel. This limitation makes them unsuitable for traction applications where mechanical shafts are indirectly coupled through the wheel-road interaction. In such cases, even minor differences in wheel diameters would result in varying rotational speeds, ultimately leading to instability.

Nevertheless, approximately a decade ago, researchers began extending MIMM control strategies to PMSMs [5], starting with the simplest case: the Mono Inverter Dual Motor (MIDM) configuration, where a single Voltage Source Inverter (VSI) supplies two parallel-connected PMSMs. Suitable applications for MIDPMSM systems include cooling fans [6], pump drives [7] and conveyor belts [8]. Control algorithms for MIDPMSM systems are generally more complex, as they must ensure consistent steady-state speed while maintaining system stability. Several approaches have been proposed in the literature, some incorporating optimization techniques to enhance overall performance and efficiency. Mean-motor approaches [9], [10] inspired by IM control strategies, treat the two PMSMs as a single equivalent machine, characterized by the average values of speed, position, and current, without leveraging the degrees of freedom in MIDPMSM for optimization purposes. Around the same time, master–slave control strategies emerged ([11], [12]), in which only one motor is directly controlled in its d-q reference frame. Later studies introduced a global Maximum Torque Per Ampere (MTPA) optimization algorithm ([13], [14]). Even in the relatively simple case of two PMSMs, implementing MTPA remains a challenge due to the high computational burden associated with solving a quartic function. This equation can be solved analytically using Ferrari's method or numerically via iterative algorithms ([13], [14]). As an alternative, offline Look-Up Tables (LUTs) can be used, though they require significant memory capacity. Some works have demonstrated simplified MTPA implementations. For example, [15] proposed a reduced-dimension LUT that achieves the same performance as [14]. In [16], the optimal solution was obtained through a combination of a feedforward term, derived from an approximate equation, and a feedback term, provided by an integral controller. In [15], [16], a third approach—distinct from the master–slave strategy—was

Received 10 April 2025; revised 12 September 2025; accepted 6 November 2025. Date of publication 17 November 2025; date of current version 15 May 2026. Paper 2025-IDC-0720.R1, presented at the 2024 International Symposium on Power Electronics, Electrical Drives, Automation and Motion, Napoli, Italy, Jun. 19–21, and approved for publication in the IEEE Transactions on Industry Applications by the Industrial Drives Committee of the IEEE Industry Applications Society [DOI: 10.1109/SPEEDAM61530.2024.10609058]. *(Corresponding author: Ivan Spina.)*

Ivan Spina, Gianluca Brando, and Adolfo Dannier are with the Department of Electrical Engineering and Information Technology, University of Naples Federico II, 80125 Naples, Italy (e-mail: ivan.spina@unina.it; gianluca.brando@unina.it; adolfo.dannier@unina.it).

Andrea Cervone is with the Department of Electrical Engineering (ESAT), Katholieke Universiteit Leuven, 3000 Leuven, Belgium (e-mail: andrea.cervone@kuleuven.be).

Color versions of one or more figures in this article are available at https://doi.org/10.1109/TIA.2025.3634050.

Digital Object Identifier 10.1109/TIA.2025.3634050

introduced, defining the semi-sum and semi-difference of motor quantities within a mean d-q reference frame. Other proposed strategies include model predictive control ([17], [18]), the Perturb & Observe technique ([19]) and Fuzzy Logic control ([20]). Additional challenges, such as current limit calculations ([21]) and parameter sensitivity analysis ([14], [15]), have also been addressed. Furthermore, studies have demonstrated the feasibility of controlling MIDPMSM systems with interior permanent magnet motors ([22]) and with two motors having different parameters ([23], [24]).

Therefore, the control of MIDPMSM systems has been extensively studied, and sensorless implementations have also been demonstrated as feasible ([14], [16], [25]). However, for a long time, research on MIMM systems remained limited to configurations with only two PMSMs, restricting their adoption in applications requiring more than two machines and consequently limiting their industrial appeal. Only recently has the first attempt to extend MIDM control techniques to Mono Inverter Multi-PMSM (MIMPMSM) systems been proposed in [26]. The ability of a single VSI to drive multiple parallel-connected PMSMs offers a significant opportunity for system simplification, with a notable reduction in the number of required components. This potential has revived interest within the scientific community, highlighting the need for further research to address unresolved challenges. Developing more advanced control strategies could help unlock the full potential of MIMPMSM systems, making them more attractive to industry. The authors of [26] demonstrated the controllability and stability of an MIMPMSM system using a master–slave approach. Additionally, they formulated and applied MTPA calculations under predefined operating conditions. However, a generalized method capable of continuously tracking the MTPA point under varying operating conditions is still lacking. Other open challenges include optimizing system efficiency, developing a real-time algorithm suitable for microcontroller implementation, and investigating the impact of parameter variations and uncertainties on system performance and stability.

Some of these aspects were addressed in [27], where two suitable MTPA methods were investigated. However, the analysis was conducted solely through simulations under a limited set of operating conditions. While this confirmed the theoretical feasibility of the methods, it lacked experimental validation on a real test bench. For example, the Look-Up-Table (LUT) approach proposed in [27] would require a prohibitive amount of memory for a low-cost system. Furthermore, the parameter variation considered in [27] was limited to stator resistance, to which the MTPA methods demonstrated low sensitivity.

This work builds upon the theoretical considerations of [27], extending them to propose an innovative solution capable of overcoming the limitations of the aforementioned LUT approach. The method proposed in this study, named Distributed Real-Time Computation (DRTC), is suitable for implementation on an actual cost-effective control platform, as demonstrated by an extensive experimental testing campaign on a laboratory demonstrator, serving as the ultimate practical validation. This approach has been validated experimentally and compared both to a baseline approach aimed at the sole master motor optimization, and to the Perturb & Observe (P&O) approach introduced in [27]. The tests cover steady-state and transient operating conditions, step changes in load and reference speed, and various unbalanced load scenarios. In the experimental setup, the algorithms were adapted to enhance system robustness against measurement noise and other disturbances that could introduce undesired oscillations in the feedback variables. Additionally, a new numerical investigation was carried out to assess the impact of parametric uncertainties on system performance. This analysis revealed behavioral differences between methods that had not emerged in the study presented in [27].

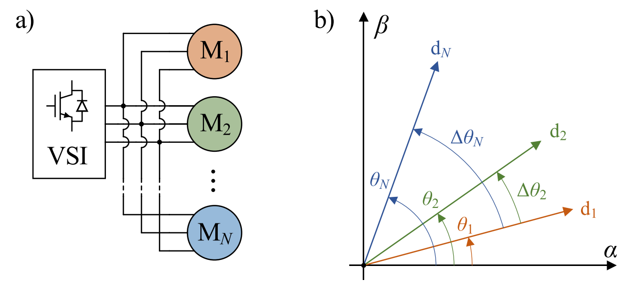

Fig. 1. (a) Architecture of the MIMPMSM system; (b) graphical representation of the relationship between the angles of the motors.

The key characteristics of the analyzed algorithms are analyzed, and their performance is compared. The results confirm the effectiveness of the proposed methods for continuously tracking the MTPA point under varying operating conditions, highlighting their distinct behaviors in terms of settling time and robustness against parameter variations.

In brief, with respect to the state of literature, and, in particular, in reference to [27], the main innovative contributions of the present work are: the proposal of an innovative method for the tracking of the MTPA; the adaptation of the general control algorithm for real-case scenario; the comparative experimental validation of all proposed methods; and a novel numerical analysis on the parameter variation impact.

The paper is organized as follows: Section II introduces the mathematical model and stability requirements. Section III details the control algorithm and MTPA strategies. Section IV validates the system through numerical and experimental results. Finally, conclusions are presented in Section V.

II. Robust Master-Slave Control of a MIMPMSM

A. Steady-state Mathematical Model

The analyzed system consists of MIMPMSM structure built upon $N \geq 3$ identical isotropic PMSMs with sinusoidal back-electromotive force (BEMF), as represented in Fig. 1(a).

Under steady-state conditions at an angular electric speed ω, the model of each machine can be conveniently expressed in its individual d, q reference frame aligned with the corresponding rotor flux as follows:

$$\begin{aligned} V_{dk} &= R_s\, I_{dk} - X_s I_{qk} \\ V_{qk} &= R_s\, I_{qk} + X_s I_{dk} + E \end{aligned} \tag{1}$$

with the following meaning for all the variables:

V_{dk}, V_{qk}: the d, q components ([Vrms]) of the stator voltages;
I_{dk}, I_{qk}: the d, q components ([Arms]) of the stator currents;
R_s: the stator resistance,
$X_s = \omega L_s$: the stator reactance, proportional to the stator inductance L_s;
$E = \omega\phi$: the BEMF amplitude ([Vrms]) linked to the flux linkage ϕ generated by the permanent magnets.

By introducing the displacement angles $\Delta\theta_k = \theta_k - \theta_1$ (where θ_k denotes the electrical angle of the k-th rotor, as illustrated in Fig. 1(b)), it is possible to refer the stator voltages of any machine M_k to the ones of first machine M_1. Since all machines are powered by the same inverter, the voltages in their respective d, q reference frames are related as:

$$\begin{aligned} V_{dk} &= V_{d1} \cdot \cos\Delta\theta_k + V_{q1} \cdot \sin\Delta\theta_k \\ V_{qk} &= V_{q1} \cdot \cos\Delta\theta_k - V_{d1} \cdot \sin\Delta\theta_k \end{aligned} \tag{2}$$

By substituting (2) into (1), the steady-state model in term of V_{d1} and V_{q1} for the MIMPMSM system is obtained:

$$\begin{aligned} V_{d1} \cdot \cos\Delta\theta_k + V_{q1} \cdot \sin\Delta\theta_k &= R_s I_{dk} - X_s I_{qk} \\ V_{q1} \cdot \cos\Delta\theta_k - V_{d1} \cdot \sin\Delta\theta_k &= R_s I_{qk} + X_s I_{dk} + E \end{aligned} \tag{3}$$

Finally, the electromagnetic torque developed by the k-th motor M_k is given by:

$$T_{ek} = \frac{3p}{\omega} \cdot E \cdot I_{qk} \tag{4}$$

where p represents the number of pole pairs of the PMSMs.

Under steady-state conditions the torque produced by each motor is equal to the mechanical load torque applied at the shaft (and it is worth emphasizing that, in general, the machines of the MIMPMSM setup can be subject to different loading torques).

At a given speed and for a fixed I_{qk}, the direct current I_{dk} of the k-th machine is a function of the applied RMS voltage magnitude V_k. Since all machines in the MIMPMSM system are powered by a common source, their RMS voltages V_k must be equal. Therefore, it results:

$$\begin{aligned} V_k^2 &= V_{dk}^2 + V_{qk}^2 = V_1^2 = V_{d1}^2 + V_{q1}^2 = \\ &= Z^2 \cdot \left(I_{dk}^2 + I_{qk}^2\right) + 2E \cdot \left(X_s I_{dk} + R_s I_{qk}\right) + E^2 \end{aligned} \tag{5}$$

The condition (5) must be verified by all the N machines, and identify some constraints on the steady-state currents of the MIMPMSM system. More specifically, as a consequence of (5), only one of the N direct axis currents I_{dk} can be freely imposed in the MIMPMSM system. Indeed, if one of the I_{dk} is imposed as a controllable degree of freedom, it will automatically determine the RMS voltages V_k which, as a consequence, will impose the current I_{dk} in all the other $(N-1)$ machines.

B. Optimal Master Selection Strategy

As demonstrated in [27], only one machine can be controlled through a closed-loop current control, while the remaining $(N-1)$ machines must operate in open-loop mode. The machine controlled in closed-loop is referred to as the *master*, whereas the remaining machines, whose behavior depends on the master's control and selection, are termed *slaves*. These motors are supplied with the same voltage and frequency as the master and are each subject to their own mechanical load. Provided that the stability conditions are satisfied, they naturally run at the same speed as the controlled motor and develop an electromagnetic torque equal to their respective load torque. For sake of simplicity and without loss of generality, the master motor is denoted with index 1, while slave motors are indexed from 2 to N. The direct axis current I_{d1} is chosen as the degree of freedom of the MIDPMSM system. Its value could be freely chosen in theory to optimize some system performances (e.g., minimizing the overall losses). However, the overall control strategy should also guarantee stability for of all the $(N-1)$ slave machines, which are operated in open loop.

As shown in [26] and recalled in [27], the stability of the system is guaranteed, regardless of the chosen if I_{d1}, if the master motor is be selected as the machine for which $\Delta T_{ek} = |T_{ek} - T_e^{sc}|$ is maximized, with $T_e^{sc} = -(3p/\omega) R_s E^2 / Z_s^2$ denoting the torque developed in short circuit condition, and $\mathbf{Z}_s = Z_s \; e^{j\varphi_s} = R_s + jX_s$ denoting the stator impedance at the angular electric speed ω. This optimal master selection strategy effectively decouples the stability requirement from the optimization of I_{d1}. As a result, I_{d1} can be freely adjusted based on the desired optimization criteria without compromising the stability of the slave machines.

It is worth noting that the master selection criterion indeed guarantees stability, but it refers to operating conditions where the system variables may change over time, yet not at an extremely fast rate. This limitation arises because the expressions resulting from the stability analysis were derived by neglecting the voltage drops associated with the current derivatives (terms of the type Ldi/dt). In a typical practical application, although the system may operate under dynamic conditions, it is not usually subjected to extremely fast transient, and in such cases the system could function without issues. On the contrary, in presence of extreme dynamic conditions the stability conditions reported in [26] and [27], alone may not be sufficient. In such case, some additional control refinements can be implemented to achieve dynamic large-scale stability, as discussed in the Appendix A.

III. Maximum Torque Per Ampere Strategy

A. Mathematical Formulation

In the proposed approach, the I_{d1} degree of freedom is exploited to minimize the overall steady-state stator losses, which are given by:

$$P^J = R_S \sum_{k=1}^{N} \left(I_{dk}^2 + I_{qk}^2\right) \tag{6}$$

Minimizing P^J for a given torque set can also be interpreted as maximizing the torque of the MIMPMSM system for a fixed equivalent RMS current. Thus, the minimization of P^J is equivalent to implementing a Maximum Torque Per Ampere (MTPA) strategy.

In (6), all steady-state quadrature currents I_{qk} are determined by the respective loading torques T_{ek} and are not influenced by I_{d1}. On the other hand, the direct currents I_{dk} of the slave machines indirectly depend on the master direct-axis current I_{d1}, as it influences the voltages applied to the system.

Contrarily to conventional PMSM drives, the optimal solution to the minimization of P^J is not generally obtained by imposing $I_{d1} = 0$, since the choice of the master current I_{d1} affects the currents I_{dk} of the slave machines according to (5). Indeed, as discussed in [27], the definition of the MTPA' solution, i.e., the value of I_{d1} which minimizes P^J for a given set $\{I_{q1},\ldots,I_{qk}\}$, requires solving a system of nonlinear equations. Finding a closed-form analytical solution is extremely challenging; thus, numerical methods must be employed for practical implementation. Nevertheless, as shown in [27], the optimal value of I_{d1} is constrained in the range $[I_d^m, 0]$, with $I_d^m = -X_s E/Z_s^2$ representing the value corresponding to the minimum applied voltage magnitude.

B. Look-Up-Table Approach

In a digital control system with a sampling time T_s, tracking the optimal master's motor direct-axis current I_d^{opt} can, in theory, be achieved using a multi-input look-up table (LUT) built offline. The LUT is populated by numerically solving the MTPA condition for a generic operating point, which is linked to the system's operating condition. However, even in a three-motor MIMPMSM configuration, an LUT-based approach would require an extensive memory allocation to store the optimal currents across different operating conditions with an acceptable resolution. In general, the number of points to be stored correspond to $res^{-(N+1)}$, where res is the resolution in pu. This memory requirement would be prohibitively large and incompatible with low-cost real-time control platforms. As an alternative, the optimal current I_d^{opt} can be computed online based on the real-time operating point. However, for larger systems (i.e., a higher number of motors), this approach can lead to significant computational complexity, requiring a high-performance control platform with increased processing power and cost, as also confirmed by the experimental results presented later in the paper. As an additional drawback, since LUT approach is entirely based on the mathematical model, it may suffer from parameters accuracy.

C. Perturb & Observe Approach

The Perturb & Observe (P&O) approach has been introduced in [27] to solve the problem of the excessive memory requirement of the LUT approach. This algorithm is implemented by updating the reference direct current I_{d1}^* by a predefined step $\Delta I_{d1}^{P\&O}$, whose sign is computed based on the cumulative joule losses P^J estimated using the expression (6) with the measured currents of the motors. As shown in [27], this method converges to the same optimal solution that would be provided with an ideal LUT based approach, and it does not show neither a heavy computational burden nor excessive memory requirements. However, since the P&O is based on the measured currents, the reference I_{d1}^* can only be updated with a relatively slow time step T_O, which is much longer than the controller time step T_s. Therefore, the convergence of the algorithm to the optimal operating conditions for the MTPA requires a relatively long settling time, especially following transient events.

D. Distributed Real-Time Computation

To address the previously discussed challenges, a new alternative approach is presented in this work. The proposed method does not aim to solve the overall optimization problem directly, which, as previously mentioned, could represent a prohibitive computational burden. Instead, it involves the computation of P^J for a trial values of i_d, representing the instantaneous d-axis current of the master motor. This approach is feasible since it does not rely on iterative methods but rather on solving a certain number of closed-form equations.

A possible strategy is to assign all potential values of i_d (properly quantized) within the range of stable operation $[i_d^m, 0]$, and compute P^J for each of them. The optimal value i_d^{opt} is then selected as the one corresponding to the minimum P^J. Naturally, attempting to perform all these calculations within a single sampling interval would still pose a computational challenge. For this reason, the optimization process can be effectively distributed across multiple sampling intervals, where, in each interval, the computation is carried out for only one trial value of i_d.

The proposed method is referred to as Distributed Real-Time Computation (DRTC) and operates as follows:

- At the start, the operating conditions of the motors (ω_r, $i_{q1},\ldots,i_{qN}$) are sampled, and the first trial value of i_d is set to i_d^m. The i_{dk} of the non-master motors are calculated via (1) and (5) and the losses using (6). The value of P^J is stored in memory along with the corresponding trial i_d value.
- At the next T_s, the value of i_d is updated by adding a resolution step Δi_d, and the computation of P^J is repeated. If, and only if, the newly computed P^J is lower than that in the previous step, the memory storing i_d and P^J values is overwritten with the updated values.
- The process terminates when the trial value of i_d reaches the upper limit of the optimal range, which is equal to 0. At this point, the stored i_d value is assumed to be i_d^{opt} and is assigned as the reference output i_d^*.

Fig. 2 illustrates the workflow of the DRTC method.

It is important to note that while the algorithm searches for the optimum point, the output i_d^* is kept constant at the value determined in the previous DRTC execution. The time required to update i_d^* is given by $T_s \cdot |i_d^m|/\Delta i_d$. However, it is generally easy to achieve acceptably short update times, even with fine resolution, especially when compared to the convergence time required by a P&O approach to reach the final value of i_d.

To further reduce the update time of i_d^*, the DRTC can alternatively be implemented as an asynchronous background task. In this case, computations take place during any available processing time within the T_s interval that is not used for other tasks.

Compared to a conventional LUT, which requires input quantization and a large amount of memory to store the precomputed optimal values, the DRTC can be regarded as an LUT

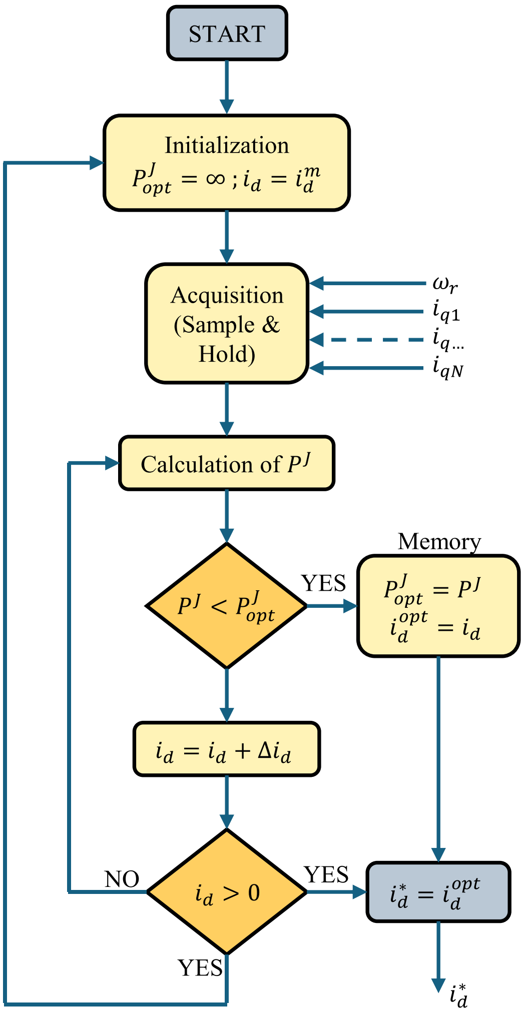

Fig. 2. Workflow of the Distributed Real-Time Computation (DRTC) method.

computed online, where the calculation is distributed across multiple sampling intervals to overcome the computational burden. For a given operating condition, described by the same input variables, the DRTC relies on the same mathematical model and parameters used to build the LUT, but instead of retrieving a pre-stored discrete value it calculates the corresponding optimal i_d^* in real time. This means that, unlike the LUT approach, the DRTC provides continuous (non-quantized) values of i_d^* and does not suffer from memory limitations. Apart from these differences, the results of the two methods are essentially identical, since both are based on the same model and parameters, and therefore exhibit the same sensitivity to parameter variations. For this reason, in this work the comparison between DRTC and LUT has been focused on their practical implementability rather than on performance, leaving more space to the more interesting comparison among DRTC and P&O.

E. Complete Control Algorithm

The complete control algorithm for the MIMPMSM system is schematically illustrated in Fig. 3, and its working principle is summarized as follows.

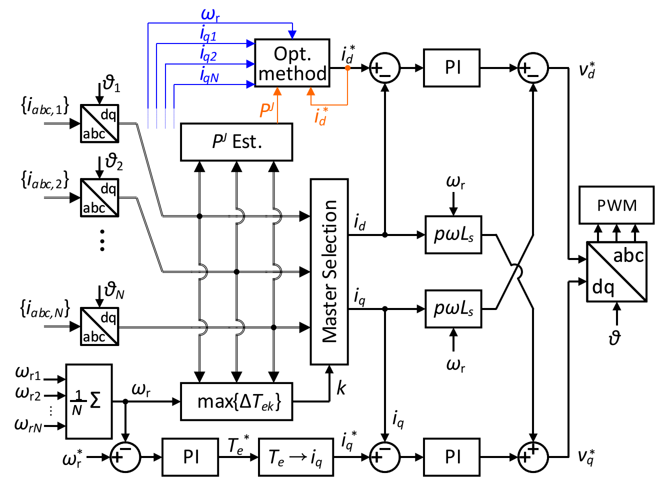

Fig. 3. Scheme of the control algorithm.

First, all the currents of the N motors are acquired and transformed into their respective $d_k q_k$ reference frames, obtaining the instantaneous values of i_{dk}, i_{qk} currents. Simultaneously, the measured speeds of all machines are averaged, and based on the resulting value ω_r, the short-circuit torque T_e^{sc} is computed.

Then, a torque estimation is performed the measured quadrature axes currents and, as explained in Section II-B, the master motor is selected based on the maximum distance ΔT_e. Considering that, depending on the operating conditions, the master motor can differ from the machine n.1 of the MIMPMSM system, in Fig. 3 and in what follows, the variables without a subscript implicitly refer to the master motor. The currents of all the machines are used to estimate the overall stator losses via (6).

Once the master motor has been selected, its currents i_d and i_q are controlled in closed-loop mode using a standard approach based on PI regulators with cross-decoupling. In this framework, the reference quadrature axis current i_q^* is generated by a standard speed control loop.

The reference direct axis current i_d^* is computed based on the selected optimization method. In this work the proposed DRTC technique is compared against P&O methods presented in [27]; In Fig. 3 the blue arrows represent the DRTC inputs, whereas the green ones refer to the P&O inputs.

Finally, the reference output voltages computed by the current controllers are transformed back into the phase variable domain and applied to the system using a standard Pulse Width Modulation (PWM) algorithm.

IV. Numerical and Experimental Validation

A. Test Bench

The considered control algorithms have been validated both numerically and experimentally. The control scheme used is based on the one shown in Fig. 3, but it has been integrated with implementation refinements aimed at enhancing robustness and stability when subjected to demanding dynamics and rejection of noise measurement. Appendix A describes these integrations in

TABLE I
PARAMETERS OF THE PMSMS

Parameter		Value
Rated Power	P_R	45 W
Rated Current	I_R	3.15 A (RMS)
Rated Speed	ω_R	3000 RPM
Phase Resistance	R_s	0.5 Ω
Phase Inductance	L_s	350 μH
Magnet Flux	ϕ	5.37 mWb
Pole Pairs	p	4

TABLE II
EXPERIMENTAL TEST SEQUENCE

Condition n.	Duration [s]	ω^* [pu]	T_{e1} [pu]	T_{e2} [pu]	T_{e3} [pu]
1	15	0.5	0.5	0	0
2	20	1	0.5	0	0
3	30	1	0.5	1	0
4	20	1	0.5	1	1
5	15	0.5	0.5	1	1
6	20	0.5	0.5	0	1

detail. The experimental setup consists of three identical PMSM from the MOTOR POWER TC 40 series, whose parameters are summarized in Table I.

The motors are driven by a SEMIKRON-SemiTeach inverter operated at 10 kHz switching frequency and controlled via a dSPACE-DS1103 control board. To generate the mechanical load, each PMSM is coupled with a DC Motor (DCM) of suitable characteristics. The latter is driven by the BOOSTXL inverter and controlled by the LAUNCHXL-F28379D, both manufactured by Texas Instruments. The DC links of both converters are powered by the same DC power supply. For proper synchronization, the braking torque values and their timing are determined by the DS1103 and sent to the LAUNCHXL via analog signals. The sampling frequency

The laboratory prototype is shown in Fig. 4.

B. Experiments

To evaluate the effectiveness of the proposed methods, a sequence of six operating points was defined, each with different torque and speed values. The aim was not only to evaluate the performance of the system in steady-state condition, but also to assess the robustness and stability of the system under extreme dynamic conditions, with step changes in the variables. In this scenario, it was quickly realized that the stability conditions reported in [26] and [27] alone were not sufficient. For this reason, the control algorithm has been integrated with implementation refinements described in Appendix A. The experimental sequence is summarized in Table II.

Conditions 1 and 2 are necessary to start the system and verify the response to speed changes with an unbalanced load. Condition 3 involves a change of the master motor. Condition 4, which is particularly critical, places two motors at full mechanical power, potentially leading to uncertainty in master attribution. Condition 5 aims to assess the system's response to speed changes in the presence of master motor uncertainty. Condition 6 reestablishes the uniqueness of the master. The sequence was executed for both previously discussed optimization methods (P&O and DRTC). Additionally, to establish a reference case, the same sequence was also performed when the PMSM control algorithm was set in a traditional manner, setting the direct-axis current to zero. Naturally, this does not constitute an optimal method for the three-motor system, as it only seeks to minimize the losses of the master motor. For this reason, this method is referred to as the "Master MTPA method" (M-MTPA).

Since the N motors may have different rotor positions at standstill, a dedicated start-up procedure aimed at aligning their magnetic axes is applied before enabling the operating conditions reported in Table II, to avoid synchronization issues. One motor is randomly selected as master, and a slowly increasing i_{d1}^* is imposed until it reaches its nominal value (with i_{q1}^* kept at zero). Then the reference angle is gradually increased from zero to 4π (two mechanical revolutions). This causes the motors to rotate slowly and align their magnetic axes with the imposed reference. In typical applications, the load torques generally increase with speed and are therefore expected to be modest at such low rotational speeds, which facilitates the alignment process. At the end of this procedure, the motors are aligned, and the FOC can be safely activated with the desired speed reference. This procedure also allows the system to generate at least one reset pulse in the incremental encoders of all the N machines. Therefore, at the end of the described start-up procedure, eventual residual misalignments can still be identified, and the activation of the FOC algorithm can be disabled in case large misalignments are present (which would indicate some abnormal issue in the operation of the MIDPMSM drive). For the sake of brevity, the electrical and mechanical waveforms during the start-up are not reported here, and only those corresponding to the operating sequence are shown.

In Fig. 5, the time trends of speed and axis current components during the sequence are presented for the three considered methods (P&O, DRTC, and M-MTPA). As can be clearly observed, the M-MTPA method sets the direct-axis current of the master motor to zero. Conversely, the DRTC method selects a negative value for the i_d of the master motor, which it assigns rapidly; In this context, the time required to update i_d^* is 0.1 s, since $T_s = 100\ \mu s$; $|i_d^m| = 5$ A; $\Delta\ i_d = 5$ mA. Finally, the P&O method also reaches a negative i_d value for the master. Naturally, the P&O needs a longer period to reach the final i_d value, as it requires time to perturb and measure the lost power to converge to the minimum value.

Fig. 6 compares the power loss obtained during the time sequence for the three methods.

It is evident that the DRTC and P&O methods ensure significantly lower losses compared to the M-MTPA method. Table III highlights the reduction in power loss achieved by the LUT and P&O methods related to the M-MTPA reference case. The experimental results are consistent with the numerical findings presented in paper [27] and confirm the validity of the proposed algorithms in a real laboratory setting, without the idealizations

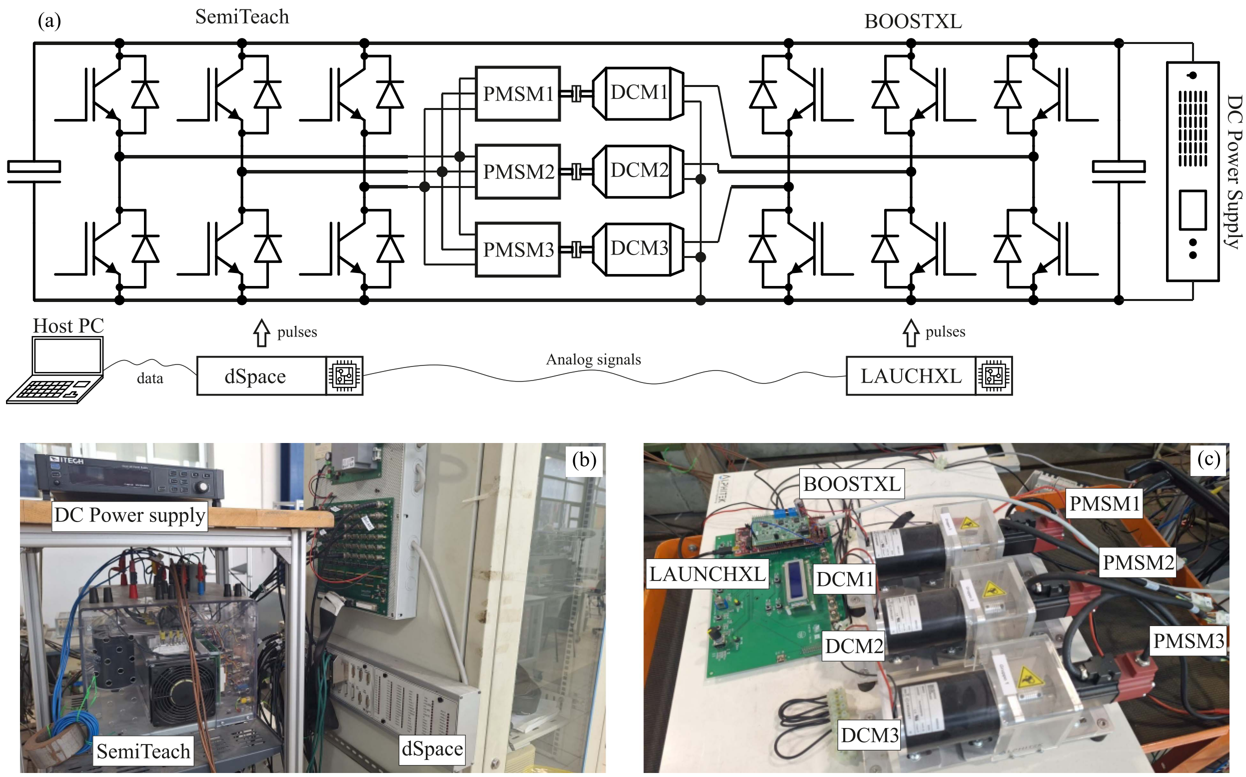

Fig. 4. Experimental setup.

TABLE III
STEADY STATE CONDITIONS POWER LOSS

Condition n.	P^J (M-MTPA)	P^J (P&O)	P^J (DRTC)
1	3,8	-23,7%	-26,3%
2	7,2	-32,1%	-32,6%
3	27,6	-32,5%	-30,3%
4	26,3	-14,3%	-13,4%
5	9,72	-11,6%	-12,0%
6	11,62	-13,8%	-14,3%

TABLE IV
MEDIAN ERROR VALUES

Condition n.	1st group median error [%] (P&O)	2nd group median error [%] (P&O)	3rd group median error [%] (P&O)	1st group median error [%] (DRTC)	2nd group median error [%] (DRTC)	3rd group median error [%] (DRTC)
1	0,022	0,022	0,016	0,419	0,419	0,437
2	0,019	0,019	0,012	1,022	1,022	0,993
3	0,044	0,044	0,044	0,170	0,166	0,128
4	0,033	0,034	0,037	0,255	0,236	0,252
5	0,011	0,011	0,010	0,541	0,527	0,488
6	0,018	0,017	0,018	0,240	0,240	0,242

TABLE V
MAXIMUM EXECUTION TIMES ON A COST-EFFECTIVE PLATFORM

M-MTPA	P&O	DRTC
76 µs	77 µs	91 µs

inherent in a simulation environment. It is worth noticing that this was not possible without the adaptation described in Appendix A. In line with [27], the analysis of the experimental results does not reveal substantial differences in the performance of the DRTC and P&O methods, except for the longer convergence times of P&O, i.e., in steady-state conditions, the two methods behave almost identically. This is also because no parametric uncertainties were introduced in the conducted tests.

C. Numerical Analysis

The behavior of the LUT approach in response to parametric variations was analyzed in [27]. However, that analysis considered only a few operating conditions and focused exclusively on uncertainties related to phase resistance. In fact, the behavior of LUT and P&O was nearly identical, with differences in power loss on the order of 1%. In this work, instead, parametric uncertainties are introduced for all the motor parameters: stator resistance and inductance, and the flux generated by the permanent magnets. Since it was not possible to alter the physical parameters of the motors in the experimental setup, this analysis was conducted numerically. The range of introduced parametric uncertainty was set to $R_s \pm 10\%$, $L_s \pm 10\%$ and $\phi \pm 5\%$. This

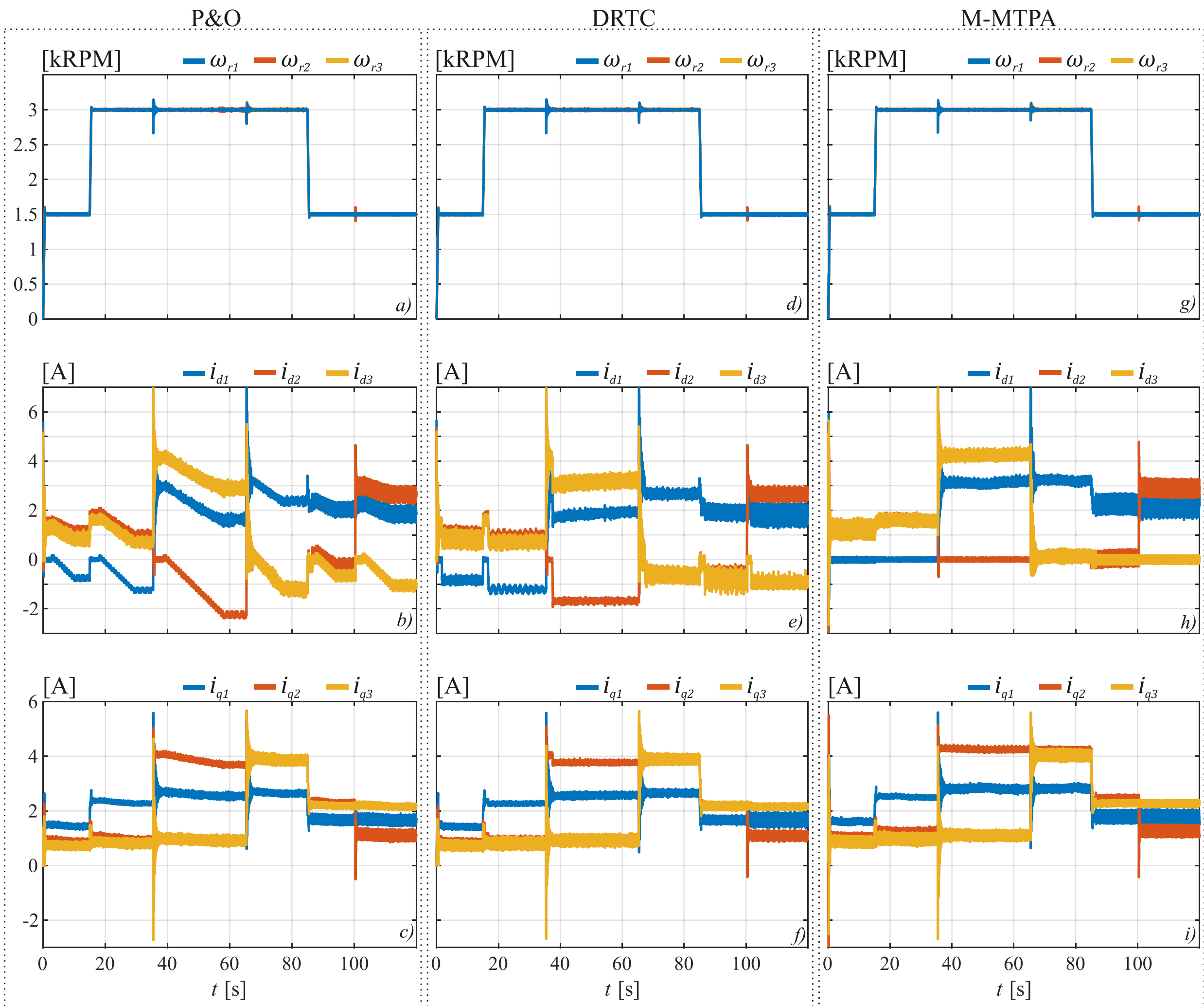

Fig. 5. Experimental time behavior of speed and currents.

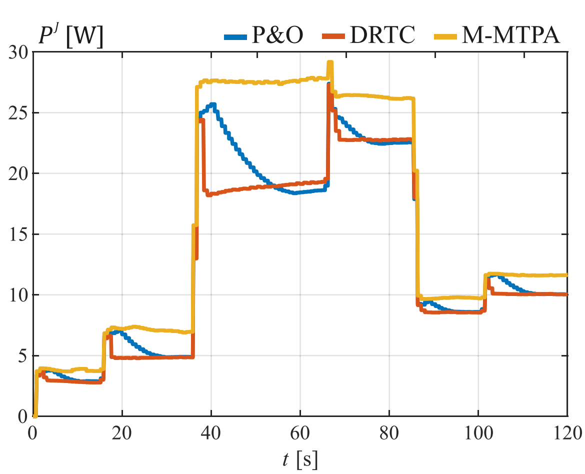

Fig. 6. Experimental power loss.

choice aligns with the confidence values reported in the datasheet of the motors used. The numerical analysis involved one hundred different simulations, each corresponding to a set of parameters randomly generated for the three motors. This approach was also aimed at testing the algorithms against potential mismatches between the actuated motors. For each simulation, the power loss values obtained by the DRTC and P&O methods at the six steady-state points of the sequence in Table II were recorded, along with the minimum achievable power loss. The latter was determined by sweeping i_d across the entire stability range. For each of the two methods, a percentage error was then computed as a measure of deviation between the obtained power loss and the minimum achievable power loss. In Fig. 7(a) and (c), the errors obtained for the DRTC and P&O methods are presented, where the 'X' symbol represents the median value computed over the one hundred data points. Based on the obtained errors, the corresponding Cumulative Distribution Function (CDF) was calculated and is shown in Fig. 7(b) and (d).

To verify the repeatability of the observed behavior, two additional groups of simulations were conducted, each consisting of 100 points, with the parameter values randomly regenerated in each case. The results confirmed the repeatability of the behavior, as evidenced by Table IV, which reports the median error values for the three simulation groups.

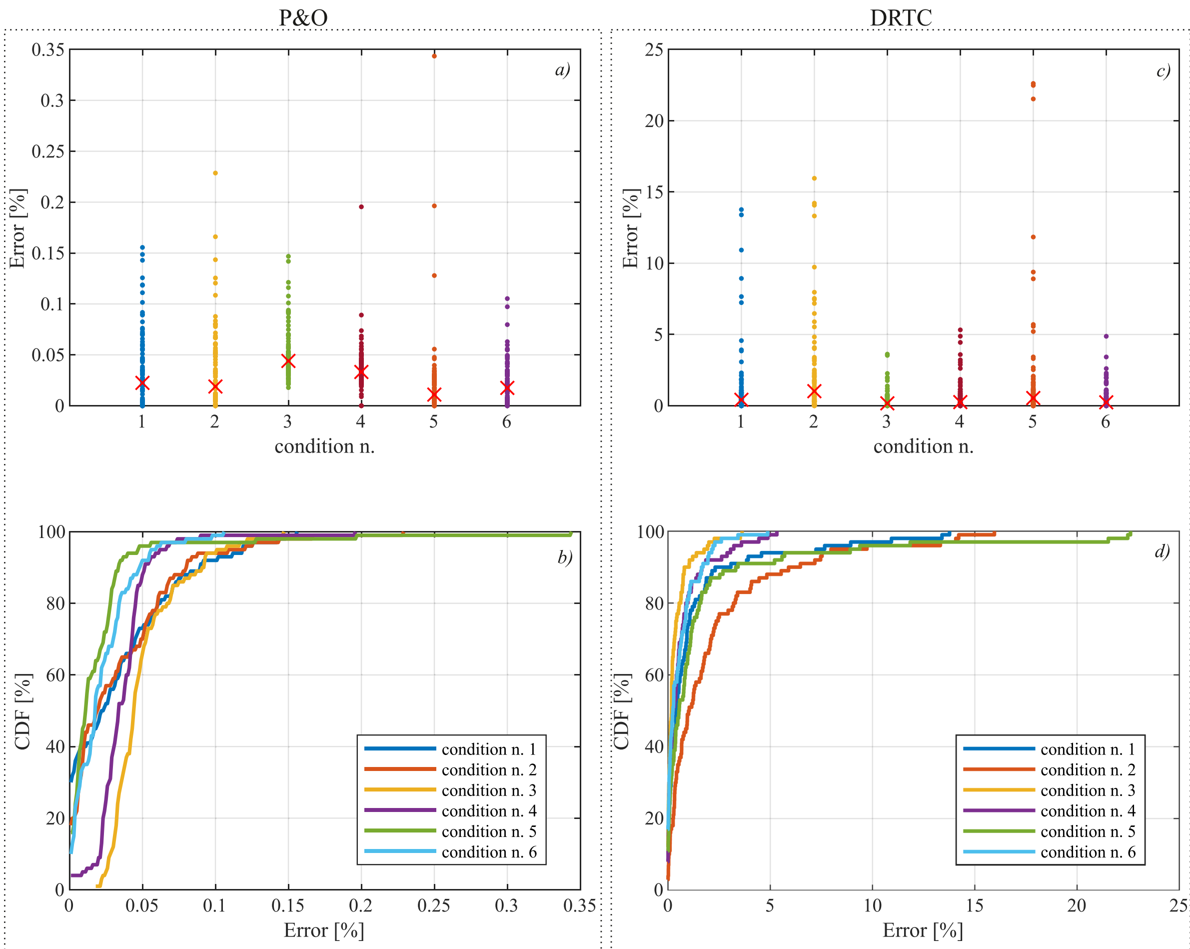

Fig. 7. Numerical analysis of parametric uncertainties.

The collected results reveal a substantial difference between the DRTC and P&O methods. While both ensure relatively low median error values, the DRTC method exhibits some instances of significant error, meaning that the obtained power losses deviate considerably from the minimum achievable values. This does not occur with the P&O method. This difference is also evident from the cumulative distribution functions (CDFs). For the P&O method, the error remains below 0.35% in 100% of cases. Conversely, for the DRTC method, if a reasonably small error threshold is set, for example, $\leq$5%, this condition is met only in 88% of the cases. The reason for this different behavior lies in the fact that the DRTC method is entirely based on the mathematical model of the system and, as such, is influenced by its parameters accuracy. On the other hand, the P&O method operates in a closed-loop manner, adapting its output based on the power loss measurement feedback. Its objective function coincides, up to a constant factor R_s, with the sum of the squared currents of all motors. As a result, uniform variations of R_s across all motors cause only a rigid shift of P^J and do not affect the optimal i_d^*. Conversely, if R_s varies differently from motor to motor, the function minimized by P&O no longer matches the true losses, which explains the modest but acceptable sensitivity observed in the numerical analysis.

D. Cost-Effective Platform Implementation

As detailed in Section IV.A, the proposed algorithms were implemented on a high-performance control platform (dSPACE-DS1103). This choice was primarily dictated by the compatibility of the available laboratory voltage and current transducers with the platform's ADC modules. However, to evaluate the feasibility of deploying the proposed methods on cost-effective systems, the P&O and DRTC algorithms were flashed onto a Texas Instruments LAUNCHXL board. The corresponding computational burden was assessed by measuring calculation times, as reported in Table V.

As can be observed, with an available sampling interval T_s of 100 μs, the M-MTPA method exhibits the lowest computational time, which practically corresponds to the execution of the basic control algorithm. The P&O method shows a similar time since it only adds the computation of P^J. Conversely, DRTC must solve the nonlinear system equations for the calculation of i_{d2} and i_{d3} corresponding to one trial value of i_{d1}, and then evaluate the associated P^J. This explains the increase of about 15 μs compared to the other two methods, which corresponds to the time required by the employed platform to solve the mathematical model of the system in the case of three motors. This result clearly shows the impracticality of adopting a real-time LUT, since in that case the same calculation would have to be repeated multiple times to identify the i_d^* that minimizes P^J, leading to a computational time exceeding T_s.

Nevertheless, although the DRTC computation time is the longest, it remains well below the available sampling interval T_s. As previously explained, the DRTC requires 0.1 s to update i_d^*, as it follows a brute-force approach, meaning all trial values of i_d^* are examined (1000 iterations). Naturally, by leveraging the monotonicity of P^J as a function of i_d, one could adopt an optimization search algorithm that assigns the next trial i_d based on the variation of P^J, thereby significantly reducing the number of iterations.

As an illustrative example, in this paper a Secant method has been considered to speed up the convergence to the optimal i_d^*. The Secant algorithm exploits the monotonic relationship between the total Joule losses P^J and the master current i_d by iteratively estimating the root of $\partial P^J/\partial i_d = 0$. In practice, the search is initialized with two trial values inside the interval $[i_d^m, 0]$, and at each iteration the current guess is updated according to the secant of the gradient function. This procedure allows the optimum to be approached without scanning the whole admissible range, as required by the brute-force DRTC implementation.

The effectiveness of this numerical optimization has been experimentally assessed under the six operating conditions reported in Table II. The number of iterations required to reach the optimal i_d^* was very limited, namely: 3, 6, 5, 5, 4, and 3 iterations for Conditions 1 to 6, respectively. Such results confirm that the optimum can be found in just a few steps, drastically reducing the computational burden compared to the brute-force DRTC approach, which required 1000 iterations corresponding to an update time of 0.1 s. With the Secant method, the update of i_d^* is instead achieved within a negligible computational time with respect to the control sampling period.

To explore an alternative approach for reducing the update time of i_d^* in the DRTC algorithm, the computation was offloaded to an asynchronous background task. The total execution time of this background task reached a maximum of 6.8 ms. Given that the synchronous task has an average residual time of 23 μs, this allows for approximately 300 sampling cycles to determine the optimum. As a result, i_d^* is updated every 0.03 s instead of 0.1 s.

Therefore, the presented results highlight that the proposed DRTC scheme can be effectively combined with lightweight numerical optimization routines, thus overcoming one of the major limitations originally pointed out for brute-force searching, and enabling a faster and more efficient real-time tracking of the MTPA point.

V. Conclusion

This paper has presented an innovative methodology named Distributed Real-Time Computation (DRTC) for the continuous tracking of the Maximum Torque Per Ampere (MTPA) condition in Mono Inverter Multi Permanent Magnet Synchronous Motors (MIMPMSM) architectures. A key advantage of the proposed approach lies in its intrinsic suitability for implementation on real-world, cost-effective platforms, effectively addressing one of the main drawbacks associated with the conventional Look-Up-Table (LUT) technique - namely, its excessive memory requirements, which can be prohibitively large for practical applications.

To thoroughly assess the performance of the proposed method, an extensive numerical and experimental campaign was conducted, comparing its effectiveness against a Perturb & Observe (P&O) approach. In pursuit of this goal, the general control framework was meticulously adapted for real-world deployment and implemented on a dedicated laboratory prototype, ensuring enhanced system robustness in the presence of measurement noise and other disturbances. Within this investigative framework, the analysis encompassed a broad spectrum of operating conditions, including steady-state and transient scenarios, abrupt variations in load and reference speed, as well as a range of unbalanced load conditions. Additionally, the impact of parametric uncertainties on system performance was systematically evaluated.

The results of the experimental study underscored both the advantages and limitations inherent to each of the considered approaches. One of the most significant distinctions between the two methods is that, while P&O demonstrated lower sensitivity to variations in motor parameters, it required a longer settling time to reach the new steady-state optimum following a step change. In contrast to traditional control strategies - typically designed to minimize stator losses for individual motors - the proposed methods yielded a significant reduction in total system losses, exceeding 32% under certain conditions. Moreover, even in the worst-case scenario characterized by substantial parameter uncertainties, the median tracking error remained exceptionally low, at approximately 1%.

Furthermore, motivated by the monotonic behavior of the loss function with respect to the master current, this paper has also exemplified the use of a Secant search method as an alternative to the brute-force scanning embedded in the DRTC. Experimental results demonstrated that the optimum can be found in only 3–6 iterations, thereby reducing the update time of optimum point to a virtually negligible computation time.

Ultimately, the experimental validation campaign provided compelling evidence of the practical effectiveness of the proposed algorithms in accurately tracking the optimal operating point of MIMPMSM systems. Their robustness was confirmed under a diverse range of steady-state and transient conditions, as well as in the presence of parameter variations, thereby demonstrating their suitability for real-world applications.

Potential future developments could include expanding the methodology to accommodate motors with different parameter configurations, exploring the application to anisotropic motor topologies, and investigating sensorless control strategies to further enhance system adaptability and efficiency.

Appendix A

The experimental tests highlighted some critical conditions where the proposed approach exhibited poor performance and/or stability problems caused either by measurement noise or heavy transient conditions. These issues have been addressed by modifying the master selection and P&O algorithms and by introducing a supervision procedure.

A. Master Selection Algorithm

Ideally, the master should be selected as the motor characterized by the greater instantaneous load factor. This approach, while effective in a simulation environment, could lead to a continuous and undesired switching of the master motor when two or more motors are characterized by similar values of the load factors and the load factors estimations are affected by a not negligible noise measurement. A low pass filter significantly attenuates the problem, but it does not fully address the issue unless a very small cut frequency is chosen, which could lead to an unstable system. Instead, a relay-based processing has been formulated and implemented as discussed below.

Firstly, the hence defined motors' normalized load factors u_k are computed as:

$$u_k = \left|T_{e,k} - T_e^{sc}\right| / T_{e,L} \tag{7}$$

with $T_{e,L}$ the reference torque limit. The normalized load factors are then processed by a relay logic which switches the master when the following condition is satisfied:

$$u_{k^*} > u_1 + \Delta \mathrm{u} \tag{8}$$

with Δu the trigger threshold and u_{k^*} the maximum slaves' load factor:

$$u_{k^*} = \max\{u_2, \ldots, u_N\} \tag{9}$$

When (8) applies, the master is switched to the slave linked to the $k*$ index (i.e., u_1 gets linked to its load factor) and the selection is held until the next overthrow of the threshold.

B. P&O Algorithm

The P&O algorithm updates the reference of the master' direct current based on the increase/decrease of the whole joule power losses. Generally, a small value of the perturbation quantity (i.e., the variation of the direct current reference) is preferred over a great one since it would lead to a smaller oscillation of the direct current reference in steady-state operation. However, in a real setup, the resultant losses variations become comparable with the oscillations introduced by the measurement noise when the direct current reference is within a suitable range of the optimal value. This could lead to a significant low frequency oscillation in the direct current reference in steady-state operation. This issue has been addressed by integrating into the P&O algorithm a hysteresis-based logic, which has been formalized by a two-level controller with output λ_P:

$$\begin{cases} |\Delta P(nT_O)| > \Delta P_H \Rightarrow \lambda_P\ (nT_O) = 1 \\ |\Delta P(nT_O)| < \Delta P_L \Rightarrow \lambda_P\ (nT_O) = 0 \\ \Delta P_L \le |\Delta P(nT_O)| \le \Delta P_H \Rightarrow \lambda_P(nT_O) = \\ \quad = \lambda_P((n-1)T_O) \end{cases} \tag{10}$$

with ΔP_H and ΔP_L the high and low hysteresis bands. λ_P allows to discriminate through an operating condition either far ($\lambda_P = 1$) or close ($\lambda_P = 0$) to the optimal one. The behavior of the algorithm is modified accordingly:

$$\begin{cases} \lambda_P(nT_O) = 1 \Rightarrow \Delta I*(nT_O) = \Delta I*(nT_O) \\ \lambda_P(nT_O) = 0 \Rightarrow \Delta I*(nT_O) = -\Delta I*(nT_O) \end{cases} \tag{11}$$

with $\Delta I*$ the increment on the direct current reference applied by the modified algorithm. As per (11), the P&O procedure follows the standard logic if the operating condition is far from the optimal one. Otherwise, the reference is continuously switched to hold the operating condition while being able to detect a departure from the optimal one.

C. Supervision Procedure

The resultant algorithm, formalized in [27] just through the definition of the master selection and MTPA procedures, has been further modified by introducing a supervision procedure which affects the whole process based on the discrimination of the current system operation between a steady-state and a transient one. The discrimination is performed by processing the maximum error ε_ω between the electrical speed reference $\omega*$ and the actual electrical speeds ω_k of the motors:

$$\varepsilon_\omega = \max\{|\omega * -\omega_1|, \ldots, |\omega * -\omega_N|\} \tag{12}$$

ε_ω is exploited to change the relay-based logic quantity λ_T (which is held to 1 in transient operation, to 0 in steady-state operation) by the following logic:

λ_T is set when ε_ω exceeds the transient threshold $\Delta\varepsilon_T$;

λ_T is cleared when ε_ω remains within the steady-state threshold $\Delta\varepsilon_R$ for a time interval greater than a specified steady-state time interval T_R.

When $\lambda_T = 0$, the algorithm proceeds normally. When $\lambda_T = 1$, the MTPA is bypassed, and the reference direct current is set to zero. This helps to increase the stability of the slaves when heavy perturbations occur.

References

[1] J. Okabe, A. Kumamoto, and Y. Hirane, "Independent closed-loop control of two induction motors paralleled to a single inverter and its applications to an automatically guided carrier vehicle," in *Proc. Ind. Electron. Conf.*, 1984, pp. 180–185.

[2] B. Wu, S. B. Dewan, and P. C. Sen, "A modified current-source inverter (MCSI) for a multiple induction motor drive system," *IEEE Trans. Power Electron.*, vol. 3, no. 1, Jan. 1988, doi: 10.1109/63.4326.

[3] P. M. Kelecy and R. D. Lorenz, "Control methodology for single inverter, parallel connected dual induction motor drives for electric vehicles," in *Proc. Power Electron. Specialists Conf.*, 1994, vol. 2, pp. 987–991, doi: 10.1109/PESC.1994.373800.

[4] P. Ghani, M. Arasteh, and H. R. Tayebi, "Analysis of electromechanical model of traction system with single inverter dual induction motor," in *Proc. 7th Power Electron., Drive Syst. Technol. Conf., Aug. 2016*, pp. 99–104, doi: 10.1109/PEDSTC.2016.7556845.

[5] M. S. D. Acampa, A. Del Pizzo, and D. Iannuzzi, "Optimized control technique of single inverter dual motor AC-brushless drives," in *Proc. 43rd Int. Universities Power Eng. Conf.*, Padua, Italy, 2008, pp. 1–6, doi: 10.1109/UPEC.2008.4651659.

[6] X. Xu, G. Zhou, J. Rao, and G. Yang, "Study and design of low-speed direct-driven permanent magnet synchronous machines(PMSM) for fan used on power air cooling island," in *Proc. 2017 20th Int. Conf. Elect. Machines Syst., 2017*, pp. 1–5, doi: 10.1109/ICEMS.2017.8056055.

[7] M. Dubey, S. Sharma, and R. Saxena, "Solar power based water pump employing Z-source inverter for PMSM drive," in *Proc. India Int. Conf. Power Electron.,* 2018, pp. 1–5, doi: 10.1109/IICPE.2018.8709405.

[8] D. Xiao and H. Shan, "Performance evaluation of dual-motor driving system for pipe belt conveyor based on current tracking master-slave control," in*Proc. Chin. Control Decis. Conf., 2019*, pp. 2540–2545, doi: 10.1109/CCDC.2019.8833227.

[9] M. S. D. Acampa, A. Del Pizzo, D. Iannuzzi, and I. Spina, "Predictive control technique of single inverter dual motor AC-brushless drives," in *Proc. Int. Conf. Elect. Machines*, 2008, pp. 1–6, doi: 10.1109/ICELMACH.2008.4800082.

[10] J. M. Lazi, Z. Ibrahim, M. H. N. Talib, and R. Mustafa, "Dual motor drives for PMSM using average phase current technique," in *Proc. IEEE Int. Conf. Power Energy*, 2010, pp. 786–790, doi: 10.1109/PECON.2010.5697686.

[11] D. Bidart, M. Pietrzak-David, P. Maussion, and M. Fadel, "Mono inverter dual parallel PMSM - structure and control strategy," in *Proc. Ind. Electron. Conf.*, 2008, pp. 268–273, doi: 10.1109/IECON.2008.4757964.

[12] A. Del Pizzo, D. Iannuzzi, and I. Spina, "High performance control technique for unbalanced operations of single-VSI dual-PM brushles motor drives," in *Proc. IEEE Int. Symp. Ind. Electron.*, 2010, pp. 1302–1307, doi: 10.1109/ISIE.2010.5637058.

[13] T. Liu and M. Fadel, "An efficiency-optimal control method for mono-inverter dual-PMSM systems," *IEEE Trans. Ind. Appl.*, vol. 54, no. 2, pp. 1737–1745, Mar./Apr. 2018, doi: 10.1109/TIA.2017.2768535.

[14] Y. Lee and J. I. Ha, "Control method for mono inverter dual parallel surface-mounted permanent-magnet synchronous machine drive system," *IEEE Trans. Ind. Electron.*, vol. 62, no. 10, pp. 6096–6107, Oct. 2015, doi: 10.1109/TIE.2015.2420634.

[15] G. Brando, L. Piegari, and I. Spina, "Simplified optimum control method for Monoinverter dual parallel PMSM drive," *IEEE Trans. Ind. Electron.*, vol. 65, no. 5, pp. 3763–3771, May 2018, doi: 10.1109/TIE.2017.2758751.

[16] G. Brando, A. Cervone, A. Del Pizzo, and I. Spina, "Sensorless control of single-inverter dual-motor ac brushless drives," in *Proc. Int. Symp. Sensorless Control Elect. Drives, 2017*, pp. 173–180, doi: 10.1109/SLED.2017.8078449.

[17] N. L. Nguyen, M. Fadel, and A. Llor, "A new approach to predictive torque control with dual parallel PMSM system," in *Proc. IEEE Int. Conf. Ind. Technol.*, 2013, pp. 1806–1811, doi: 10.1109/ICIT.2013.6505950.

[18] A. Cervone, L. P. Di Noia, R. Rizzo, I. Spina, and R. Miceli, "A constrained optimal model predictive control for mono inverter dual parallel PMSM drives," in *Proc. 7th Int. IEEE Conf. Renewable Energy Res. Appl., 2018*, pp. 1501–1507, doi: 10.1109/ICRERA.2018.8567021.

[19] J. Lee and J. W. Choi, "MTPA control method for MIDP SPMSM drive system using angle difference controller and P&O algorithm," *IEEE Trans. Power Electron.*, vol. 37, no. 12, pp. 15382–15396, Dec. 2022, doi: 10.1109/TPEL.2022.3196400.

[20] J. M. Lazi, Z. Ibrahim, M. Sulaiman, F. A. Patakor, and S. N. M. Isa, "Fuzzy logic speed controller with reduced rule base for dual PMSM drives," *World Acad. Sci. Eng. Technol.*, vol. 77, pp. 252–257, 2011.

[21] A. Cervone, L. P. Di Noia, R. Rizzo, and I. Spina, "A novel current references limitation strategy in mono-inverter dual PMSM drives," in *Proc. Int. Conf. Elect. Machines, 2018*, pp. 1353–1359, doi: 10.1109/ICELMACH.2018.8507240.

[22] Y. Lee and J. I. Ha, "Control method for mono inverter dual parallel interior permanent magnet synchronous machine drive system," in *Proc. IEEE Energy Convers. Congr. Expo.,* 2015, pp. 5256–5262, doi: 10.1109/ECCE.2015.7310399.

[23] M. M. Boroujeni and G. A. Markadeh, "Energy-based control technique for monoinverter dual parallel PMSM with different parameters," *IEEE Trans. Ind. Electron.*, vol. 69, no. 12, pp. 12162–12172, Dec. 2022, doi: 10.1109/TIE.2021.3134051.

[24] T. Liu, Z. Liu, and F. Zhu, "A nonlinear robust speed controller for dual nonidentical parallel PMSM system," *IEEE Trans Power Electron*, vol. 37, no. 9, pp. 10190–10199, Sep. 2022, doi: 10.1109/TPEL.2022.3157140.

[25] A. Asri, D. Ishak, S. Iqbal, and M. Kamarol, "A speed sensorless field oriented control of parallel-connected dual PMSM," in *Proc. IEEE Int. Conf. Control Syst., Comput. Eng., 2011*, pp. 567–570, doi: 10.1109/ICCSCE.2011.6190590.

[26] T. Liu, M. Fadel, J. Li, and X. Ma, "A MTPA control strategy for mono-inverter multi-PMSM system," *IEEE Trans. Power Electron.*, vol. 36, no. 6, pp. 7165–7177, Jun. 2021, doi: 10.1109/TPEL.2020.3038797.

[27] I. Spina, G. Brando, and A. Cervone, "A perturb-and-observe based MTPA algorithm for mono-inverter multi PMSM electric drives," in *Proc. Int. Symp. Power Electron., Elect. Drives, Automat. Motion*, 2024, pp. 169–177, doi: 10.1109/SPEEDAM61530.2024.10609058.

Ivan Spina (Member, IEEE) received the M.S. (*cum laude*) and Ph.D. degrees in electrical engineering from the University of Naples Federico II, Naples, Italy, in 2008 and 2012, respectively. He was a Postdoctoral Fellow from 2012 to 2013, Assistant Professor from 2014 to 2020, and Research Fellow with the Birmingham Centre for Railway Research and Education Birmingham, U.K., in 2017. Since 2018, he has been teaching in Urban Railway Engineering program with the University of Birmingham, Singapore. He is currently an Associate Professor of electrical machines and drives with University of Naples Federico II. His research interests include modeling, diagnostics, control of power electronics, electrical drives for industrial and traction applications.

Gianluca Brando was born in Naples, Italy, on Sep. 27, 1973. He received the M.S. (*cum laude*) and Ph.D. degrees in electrical engineering from the University of Naples Federico II, Naples, Italy, in 2000 and 2004, respectively. He was a Postdoctoral Research Fellow with the Department of Electrical Engineering, University of Naples Federico II, from 2000 to 2012, and Assistant Professor with the Department of Electrical Engineering and Information Technology, University of Naples Federico II, from 2013 to 2020. Since 2020, he has been an Associate Professor of electrical machines and drives with the Department of Electrical Engineering and Information Technology, University of Naples Federico II.

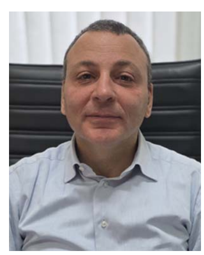

Adolfo Dannier (Senior Member, IEEE) received the M.Sc. degree (*cum laude*) and Ph.D. degrees in electrical engineering from the University of Naples Federico II, Naples, Italy, in 2003 and 2008, respectively. Since 2020, he has been an Associate Professor with the University of Naples Federico II, where he teaches courses on electric machines, power electronic converters, electrical technologies for mobility, and energy storage systems. His research interests include multilevel converters, fault-tolerant architectures, high-performance drives with permanent-magnet motors, power conversion systems, and energy storage solutions for electric vehicles and renewable energy integration. He has contributed to numerous national and international research projects and authored a significant number of scientific publications in these areas.

Andrea Cervone (Member, IEEE) received the B.Sc., M.Sc., and Ph.D. degrees in electrical engineering from the University of Naples Federico II, Naples, Italy, in 2014, 2017, and 2021, respectively. From 2021 to 2024, he was a Postdoctoral Researcher with the Power Electronics Laboratory, EPFL, Switzerland. Since 2024, he has been an Assistant Professor with the Department of Electrical Engineering of KU Leuven, Leuven, Belgium. His research interests include modeling and control of power electronic converters and electric drives, solid-state transformers, multilevel converters, and multiphase electric drives. Dr. Cervone is an Associate Editor for IEEE Transactions on Industrial Electronics.